Received: 18 July 2024 | Revised: 27 September 2024 | Accepted: 30 September 2024

DOI: 10.1111/dgd.12946

RESEARCH ARTICLE

DGD Development, Growth & Differentiation | JSDB Japanese Society of Developmental Biologists | WILEY

Mitochondrial DNA replication is essential for neurogenesis but not gliogenesis in fetal neural stem cells

Meri Walter-Manucharyan[1] | Melanie Martin[2] | Julia Pfützner[1] | Franz Markert[3] | Gerhard Rödel[4] | Andreas Deussen[2] | Andreas Hermann[1,5,6,7] | Alexander Storch[1,3,5,7]

[1]Division of Neurodegenerative Diseases, Department of Neurology, Technische Universität Dresden, Dresden, Germany

[2]Department of Physiology, Technische Universität Dresden, Dresden, Germany

[3]Department of Neurology, University of Rostock, Rostock, Germany

[4]Institute of Genetics, Technische Universität Dresden, Dresden, Germany

[5]Center for Regenerative Therapies Dresden, Dresden, Germany

[6]Translational Neurodegeneration Section "Albrecht Kossel", Department of Neurology, University of Rostock, Rostock, Germany

[7]German Center for Neurodegenerative Diseases (DZNE) Rostock/Greifswald, Rostock, Germany

Correspondence
Franz Markert, Department of Neurology, University of Rostock, Gehlsheimer Strasse 20, 18147 Rostock, Germany.
Email: franz.markert@med.uni-rostock.de

Funding information
Zentrum für Regenerative Therapien Dresden; Hermann und Lilly Schilling-Stiftung für Medizinische Forschung; Medizinische Fakultät Carl Gustav Carus, Technische Universität Dresden; Advocacy for Neuroacanthocytosis Patients

Communicating Editor: Tatsumi Hirata

Abstract

Mitochondria are unique organelles that have their own genome (mtDNA) and perform various pivotal functions within a cell. Recently, evidence has highlighted the role of mitochondria in the process of stem cell differentiation, including differentiation of neural stem cells (NSCs). Here we studied the importance of mtDNA function in the early differentiation process of NSCs in two cell culture models: the CGR8-NS cell line that was derived from embryonic stem cells by a lineage selection technique, and primary NSCs that were isolated from embryonic day 14 mouse fetal forebrain. We detected a dramatic increase in mtDNA content upon NSC differentiation to adapt their mtDNA levels to their differentiated state, which was not accompanied by changes in mitochondrial transcription factor A expression. As chemical mtDNA depletion by ethidium bromide failed to generate living ρ° cell lines from both NSC types, we used inhibition of mtDNA polymerase-γ by 2′-3′-dideoxycytidine to reduce mtDNA replication and subsequently cellular mtDNA content. Inhibition of mtDNA replication upon NSC differentiation reduced neurogenesis but not gliogenesis. The mtDNA depletion did not change energy production/consumption or cellular reactive oxygen species (ROS) content in the NSC model used. In conclusion, mtDNA replication is essential for neurogenesis but not gliogenesis in fetal NSCs through as yet unknown mechanisms, which, however, are largely independent of energy/ROS metabolism.

KEYWORDS
differentiation, gliogenesis, mtDNA, neural stem cells, neurogenesis

1 | INTRODUCTION

Mitochondria are essential membrane-bound cell organelles that play a pivotal role in many cellular processes including fatty acid oxidation, ion homeostasis, Fe-S cluster formation, oxygen sensing, apoptosis, and biosynthesis of essential molecules such as pyrimidine and heme (Figge et al., 2012, McBride et al., 2006, Nesti et al., 2007, Scarpulla, 2008b). They have their own genome, the mitochondrial DNA (mtDNA), which resides in the mitochondrial matrix together with mitochondrial ribosomes, transfer RNAs (tRNAs), and a highly

concentrated mixture of enzymes, required for mitochondrial function such as the tricarboxylic acid cycle and β-oxidation (Attardi, 1985). The mtDNA encodes only a small number of genes necessary for the molecular architecture and biological function of the organelle. Because of this limitation, mitochondria are considered as semi-autonomous in a sense that they mainly rely on the expression of nuclear encoded genes important for their biological function (Bereiter-Hahn & Voth, 1994; Figge et al., 2012; Saccone et al., 2000). For example, the vast majority of the proteins of five oxidative phosphorylation complexes in the inner membrane of mitochondria are encoded by the nuclear genome, although complexes I, III, IV, and V have at least one subunit encoded by mtDNA (Anderson et al., 1981).

The role of mitochondria was recently highlighted in the process of stem cell differentiation (Chen et al., 2008; Cho et al., 2006; Chung et al., 2007; Wanet et al., 2015). It has been reported that upon spontaneous differentiation of human embryonic stem cells (ESCs), the mitochondrial biogenesis was upregulated and the mitochondrial morphology resembled the characteristics of mature cells, which included higher mtDNA copy number and increased ATP production (Cho et al., 2006; Kristiansen et al., 2022). As a consequence, more reactive oxygen species (ROS) were produced, which led to the expression of various antioxidant enzymes such as Cu/Zn-dependent superoxide dismutase, glutathione peroxidase, and catalase. Lonergan and co-workers showed similar results in monkey stromal stem cell lines indicating that the higher ATP level per cell could serve as a signal for the loss of stemness and hence a marker for differentiation (Lonergan et al., 2006). Hence, mitochondrial biogenesis largely contributed to ATP production, which is necessary for the differentiation. This highlights the importance of mitochondria playing a crucial role in the regulation of energy metabolism during differentiation in response to higher energy demand of the cells (Chen et al., 2008; Cho et al., 2006).

In mammals, the master regulator of mitochondrial biogenesis is peroxisome proliferator-activated receptor γ co-activator α (PGC1α). It is well-known that nuclear respiratory factor 1 (NRF-1) is an important target for the mitochondrial biogenesis and its expression is induced by PGC1α. The induction of NRF-1 and NRF-2 leads to the increased expression of mitochondrial transcription factor A (TFAM), which is a direct regulator of mtDNA transcription and replication (Wu et al., 1999). Both NRF-1 and NRF-2 have been related to the transcriptional control of mitochondrial biogenesis-associated genes, particularly acting on the mtDNA transcription machinery including TFAM, mitochondrial transcription factor 1 and 2 as well as mtRNA polymerase. It was shown that NRF-1 alone or together with NRF-2 can act on the expression of nuclear genes that encode subunits for the respiratory chain complexes (Kelly & Scarpulla, 2004; Scarpulla, 2002a; Scarpulla, 2002b; Scarpulla, 2008a). Moreover, these proteins are involved in the expression of components necessary for the mitochondrial protein import and assembly apparatus.

Cho and colleagues studied mitochondrial biogenesis during spontaneous differentiation of ESCs into the three germ layers (Cho et al., 2006), making it difficult to describe metabolic changes for a specific germ layer or even cell type. A number of studies were also conducted towards a defined, lineage-specific differentiation where the changes in metabolism and mitochondrial function were described. Chen et al. showed that upon osteogenic differentiation of mesenchymal stem cells (MSCs), the mRNA expression of PGC1α mRNA was increased followed by the increase in mitochondrial mass and oxygen consumption (Chen et al., 2008). Similar results were obtained during adipogenic differentiation of human MSCs (Zhang et al., 2013). Regarding neuronal differentiation, it has been demonstrated that PGC1α effects are developmental stage-dependent with the strongest effects in the intermediate stage of early neural progenitors when compared with neural stem cells (NSCs) and advanced neuroprogenitors as derived from induced pluripotent stem cells (iPSCs) (Augustyniak et al., 2019). Furthermore, the authors showed increased mtDNA copy numbers and mRNA levels of glia-specific as well as neuron-specific markers after PGC1α induction (Cho et al., 2006). There are convincing data that both lineages depend on proper PGC1α levels (Souder et al., 2023; Zehnder et al., 2021). Potentially, various PGC1α isoforms are needed for either neuronal or glial fate decision of NSCs (Lozoya et al., 2021; Souder et al., 2023) and PGC1α could be involved specifically during early differentiation (Soares et al., 2024).

However, the regulation of mitochondrial biogenesis in NSCs during their differentiation process into neural lineages (neurons and glia) remains largely elusive. Despite progress during recent years regarding the involvement of factors in mitochondrial biogenesis, it is still not clear whether and how mtDNA itself is involved in NSC differentiation. We therefore aimed to investigate mitochondrial biogenesis during differentiation of NSCs, thereby concentrating on the role of mtDNA in this process. We have used a loss of function model, which was achieved by mtDNA depletion, to decipher mtDNA involvement during differentiation of multipotent primary NSCs as well as in glia-specific NSCs.

2 | MATERIALS AND METHODS

2.1 | Animals

Wild-type C57BL/6/J mice were purchased from Charles River (Sulzfeld, Germany) and maintained under a 12-hour/12-hour light/dark cycle with constant temperature and humidity. Food and water were available ad libitum. All animal protocols were reviewed and approved by the Animal Welfare Committee at the Technische Universität Dresden and the Landesdirektion Sachsen, Dresden, Germany (governmental authorities; no. 24-9168.24-1/2010-5).

2.2 | Isolation, expansion, and differentiation of fetal forebrain-derived NSCs

Neural stem cells (NSCs) were isolated from embryonic day (E) 14.5 mouse embryos. The dissection was performed under a dissection microscope, and the meninges were carefully removed after

cutting out the forebrain. Briefly, the forebrain-derived tissue was isolated and digested in 0.05% trypsin solution, triturated, spun down, and subsequently seeded onto poly-L-ornithine/fibronectin-coated cell culture dishes. The cells were grown in EM-1 expansion medium (Dulbecco's modified Eagle's medium [DMEM] high glucose 65% [v/v], F-12 + GlutaMAX™ 32% [v/v], B27 supplement 2% [v/v], penicillin/streptomycin 1% [v/v]) supplemented with 10 ng/mL epidermal growth factor and 10 ng/mL fibroblast growth factor-2. About 2×10^6 viable NSCs were plated in 25-cm^2 cell culture flasks and incubated at 37°C in 5% CO_2 and 95% air (21% O_2). At day 7, NSCs were cultured in differentiation medium for another 7 days. The differentiation medium was devoid of growth factors and only supplemented with 10% (v/v) fetal calf serum. To achieve mtDNA depletion, concentrations of 30 μM, 50 μM, or 100 μM of 2′-3′-dideoxycytidine (ddC) were used. ddC treatment was started at day 5 after NSC preparation and seeding. After 2 days of ddC treatment, expanding NSCs were analyzed or switched to differentiation medium. Differentiated NSCs were analyzed at differentiation day 7 (defined as 7 days after the start of the differentiation process).

2.3 | Expansion and differentiation of CGR8-NS cells

Conti and colleagues used the lineage selection technique to produce homogeneous NSC cultures including the CGR8-NS cell line (Conti et al., 2005; Li et al., 1998). It represents a pure and highly homogeneous NSC culture. CGR8-NS cells have the same characteristics as radial glial cells and express both radial glia markers and neural precursor markers such as Sox2 and Olig2, but they are negative for glial fibrillary acidic protein (GFAP). CGR8-NS cells were expanded in 0.1% gelatin coated flasks in NS basal medium which comprises Euromed-N medium 100% (v/v) (similar to the composition of DMEM) supplemented with L-glutamine 1% (v/v), penicillin/streptomycin 1% (v/v) and N-2 supplement 1% (v/v). Growth factors were added to the medium before seeding the cells (fibroblast growth factor-2 10 ng/mL and epidermal growth factor 10 ng/mL). Differentiation was performed in poly-L-ornithine/laminin-coated flasks. The medium was supplemented with fetal calf serum 1% (v/v) devoid of both growth factors. The composition of N-2 supplement differs from that of the original N-2 supplement by a higher content of insulin and bovine serum albumin (BSA). 10× N-2 supplement is composed of 6.875 mL of DMEM: F12 (L-glutamine), 1 mL of insulin (25 mg/mL), 1 mL of apo-transferrin (100 mg/mL), 1 mL BSA (75 mg/mL), 33 μL of progesterone (0.6 mg/mL), 100 μL putrescine (160 mg/mL), and 10 μL of sodium selenite (3 mM). To achieve mtDNA depletion, either 0.0625 to 0.5 μg/mL of ethidium bromide or 80 μM or 100 μM of ddC were used when seeding the cells (day 0). CGR8-NS cells were analyzed after expansion (day 2) or switched to differentiation medium. The differentiation state of CGR8-NS cells was additionally analyzed at differentiation day 1 (i.e. 1 day after the start of the differentiation process), but all further analyses were performed at differentiation day 7.

2.4 | Gene expression analysis

RNA was isolated with the "RNeasy Mini Kit" (Qiagen, Hilden, Germany) followed by treatment with RNase-free DNase according to the manufacturer's instruction. DNA isolation was performed using a "DNeasy Blood and Tissue Kit" (Qiagen). To quantify relative levels of RNA and DNA, a quantitative real-time reverse transcription-polymerase chain reaction (qRT-PCR) was performed both with the Brilliant® III Ultra QRT-PCR Master Mix Kit (Agilent Technologies, Santa Clara, CA, USA, for DNA) and SYBR® Green PCR kit (QuantiTect® for cDNA, Qiagen) according to the manufacturers' instructions. For qRT-PCR analyses, 1 μg RNA of each sample was subjected to cDNA synthesis by using oligo(dT) primers (QuantiTect®, Qiagen) and a reverse transcription kit in 20 μL of reaction volume, according to the manufacturer's protocol (QuantiTect®, Qiagen).

DNA or cDNA (from RNA samples) was amplified using 0.4–0.8 pmol/μL of both sense and antisense primer. The following cycle protocol was used: PCR was performed in a 25-μL volume containing 10 ng/μL DNA or 1 μL cDNA or dH_2O as control, 12.5 μL SYBR® Green Master Mix, 0.75 μL ROX (reference dye used 1:1000), dH_2O and 2 μL primer mix (forward and reverse primer, 5–10 pmol/μL each) under the following conditions: 95°C for 15 min, followed by 40 cycles of denaturation for 15 s at 94°C, annealing for 30 s at 54°C, and extension for 30 s at 72°C. Further denaturation of PCR products was performed for 1 min at 95°C followed by the final annealing of the PCR products for 30 s at 55°C for the generation of the dissociation curves by slowly heating the samples for 30 s at 95°C and constantly measuring the fluorescence.

The following primer sets were designed using Primer3 and BLAST (National Center of Biology Information, NCBI) and were purchased lyophilized and salt-free from Operon (Cologne, Germany; http://www.operon.com/default.aspx): *Nd1* sense: CCT TGT TCC CAG AGG TTC AA, *Nd1* antisense: CAA TGT TAG GGC CTT TTC GT; *Pop5* sense: GTT CAC TTG GGG GAC TCT GA, *Pop5* antisense: AGC GTG CCC TGT CAA TCT; *Pgc1a* sense: CAA CCG CAG TCG CAA CAT GCT, *Pgc1a* antisense: TGG GGA ACC CTT GGG GTC ATT TG; *Hmbs* sense: TCA TTG CTA TGT CCA CCA CG, *Hmbs* antisense: GAG TGA ACG ACC AGG TCC A. Primers not specified by manufacturer were from Qiagen Science: *Cat* QuantiTect®Primer Assay Mm_Cat_1_SG Cat. No. QT01058106; *Tfam* QuantiTect®Primer Assay Mm_Tfam_1_SG Cat. No. QT00154413; *Sod2* QuantiTect®Primer Assay Mm_Sod_2_1_SG Cat. No. QT00161707; *Pop5* QuantiTect®Primer Assay Mm_Pop5_va.1_SG Cat. No. QT01548428.

The formula ($2^{(Ct\ [housekeeping\ gene]\ -\ Ct\ [target\ gene])}$) of the comparative threshold cycle (ΔΔCt method) described by Livak and Schmittgen was used to quantify relative RNA/DNA levels (Livak & Schmittgen, 2001). To estimate the relative copy number of the mtDNA by qRT-PCR, the Ct value of *Nd1* was related to *Pop5*.

2.5 | Immunocytochemistry

NSCs were washed once with phosphate-buffered saline (PBS), fixed with Accustain for 45 s and then incubated in blocking solution,

containing 0.2% Triton and 3% donkey serum in PBS (1 h, room temperature). Primary antibody incubation was carried out in blocking solution at 4°C, overnight, whereas secondary antibody incubation was carried out at room temperature for 1 h. The following primary antibodies were used: mouse anti-β-III-tubulin 1:1000 (Covance, Princeton, NJ, USA), chicken anti-GFAP 1:1000 (Abcam, Cambridge, UK), rabbit anti-Nestin 1:500 (Abcam). The cell nuclei were counterstained with Hoechst 33342 (0.75 μL/mL Hoechst 33342 in PBS) for 1 min.

Mitochondria were visualized by incubating the cells in culture media containing the fluorescent probe MitoTracker® Green FM (final concentration of 75 nM), which stains mitochondria independently of their membrane potential. The incubation was carried out at 37°C for 45 min. Later, the cell nuclei were counterstained with Hoechst 33342 (0.75 μL/mL Hoechst 33342 in PBS) for 1 min. Cells were then washed with PBS and further incubated with the same medium. The stained cells were analyzed by fluorescence microscopy (DM IRE2) and images were acquired using FW4000 (both from Leica, Wetzlar, Germany). Total cell numbers and positive cells were quantified using ImageJ (NIH, Bethesda, MD, USA). A total of 1,000 to 2,500 Hoechst 33342^{+} cells per coverslip were counted and controlled for morphology. At least three coverslips were counted per condition.

2.6 | Isolation of mitochondria and Western blotting

NSCs and their differentiated derivatives were harvested using Accutase® (PAA Laboratories, Cölbe, Germany) treatment. Mitochondria were isolated from the cells by using Mitochondria Isolation Kit for Cultured Cells with Homogenizer (MitoSciences/Invitrogen, Darmstadt, Germany) following the protocol of the manufacturer. The mitochondrial suspension was shock frozen in liquid nitrogen and stored at −80°C. For immunoblot analysis, 15–20 μg of mitochondrial extracts from undifferentiated and differentiated CGR8-NS cells were mixed with 2.5 μL of sample buffer. The final volume was adjusted to 12.5 μL with H_2O. Upon denaturation of the protein by incubating the sample mixture at 95°C for 5 min, the samples were immediately put on ice and centrifuged briefly before loading the gel lanes. The NuPage® 12% Bis–Tris gels (1.0 mm × 10 wells) were washed with water and placed in an electrophoresis chamber filled with NuPage® 1× MOPS running buffer. After loading of the samples, the gel electrophoresis ran constantly at 125 V for up to 90 min. Then the proteins were transferred onto a nitrocellulose membrane according to the manufacturer's protocol. The membrane was blocked afterwards for 1 h with 5% dried milk containing PBST (1 mL Tween 20% in 1 L PBS) to prevent non-specific background binding of primary and/or secondary antibodies to the membrane. The membrane was incubated with primary antibodies against goat anti-mtTfa (herein called Tfam), 1:200, Santa Cruz Biotechnology (Dallas, TX, USA); rabbit anti-α-tubulin, 1:1000, Abcam; mouse anti-CoxIV, 1:1000, Abcam in PBST overnight at 4°C. After three washing steps the membrane was incubated with secondary antibodies diluted 1:2000 in 1% dried milk containing PBST for 1 h at room temperature (with horseradish peroxidase-conjugated donkey anti-goat, anti-rabbit and anti-mouse antibodies; Dianova Hamburg, Germany). The detection of the membrane was performed after the final washing steps by Bioimager LAS3000.

2.7 | Native nucleotide measurement

NSCs were harvested from poly-L-ornithine/fibronectin- and poly-L-ornithine/laminin-coated T-25 fLasks respectively and suspended in 300 μL of PBS. The samples were further mixed with 300 μL perchloric acid (1 mol/L) to abolish any enzymatic activity. Thereafter, 300 μL K_3PO_4 (1 mol/L) was added to neutralize the perchloric acid. The samples were centrifuged at 13,000 rpm at 4°C for 10 min to remove the salts. The supernatant was carefully pipetted into a new Eppendorf tube and immediately frozen in liquid nitrogen and then stored at −80°C for later high-performance liquid chromatography (HPLC) measurements. For derivatization, 51 μL of citrate–phosphate buffer was added to the samples. The reaction started by the addition of 5 μL chloracetaldehyde. After incubation for 40 min at 80°C, the samples were cooled down to 4°C for 20 min to stop the reaction. Derivatization is performed to convert ATP and ADP into their $1,N^6$-etheno-derivatives, denoted as ε-ATP, ε-ADP. The samples were assayed by reverse-phase separation in HPLC using Waters® Alliance 2695 and XTerra® MS C18 column. The etheno-labeled substances, such as the ε-ATP and ε-ADP, were detected by a fluorescence detector with an excitation wavelength of 280 nm and an emission wavelength of 410 nm.

2.8 | Measurement of cellular ROS content

The cellular content of ROS was measured using dihydroethidium (DHE) and CellROX® green (both Thermo Fisher Scientific, Bremen, Germany) staining in proliferating and differentiated cells using standard protocols as published for DHE (Peterson et al., 2011) or provided by the manufacturer (CellROX®; www.thermofisher.com). Microscopic images were captured using an FW4000 microscope (Leica) and quantification of fluorescence signal was done using ImageJ (NIH) and normalized to control condition for each experiment.

2.9 | Cell counting and statistics

Cell counting was performed manually by the same investigator, who was blinded for the corresponding condition. For analysis of MitoTracker intensity per cell, at least 50 cells per condition were manually surrounded using the autofluorescence of the cell bodies. An area without cells was used for background subtraction. All statistical analyses were performed using SPSS statistical software for Windows version 21. In some experiments data were normalized to control samples as described in the text. Normal distribution of data was confirmed by Kolmogorov–Smirnov testing. Differences between mean values of two groups were analyzed by Student's two-sided *t*-test.

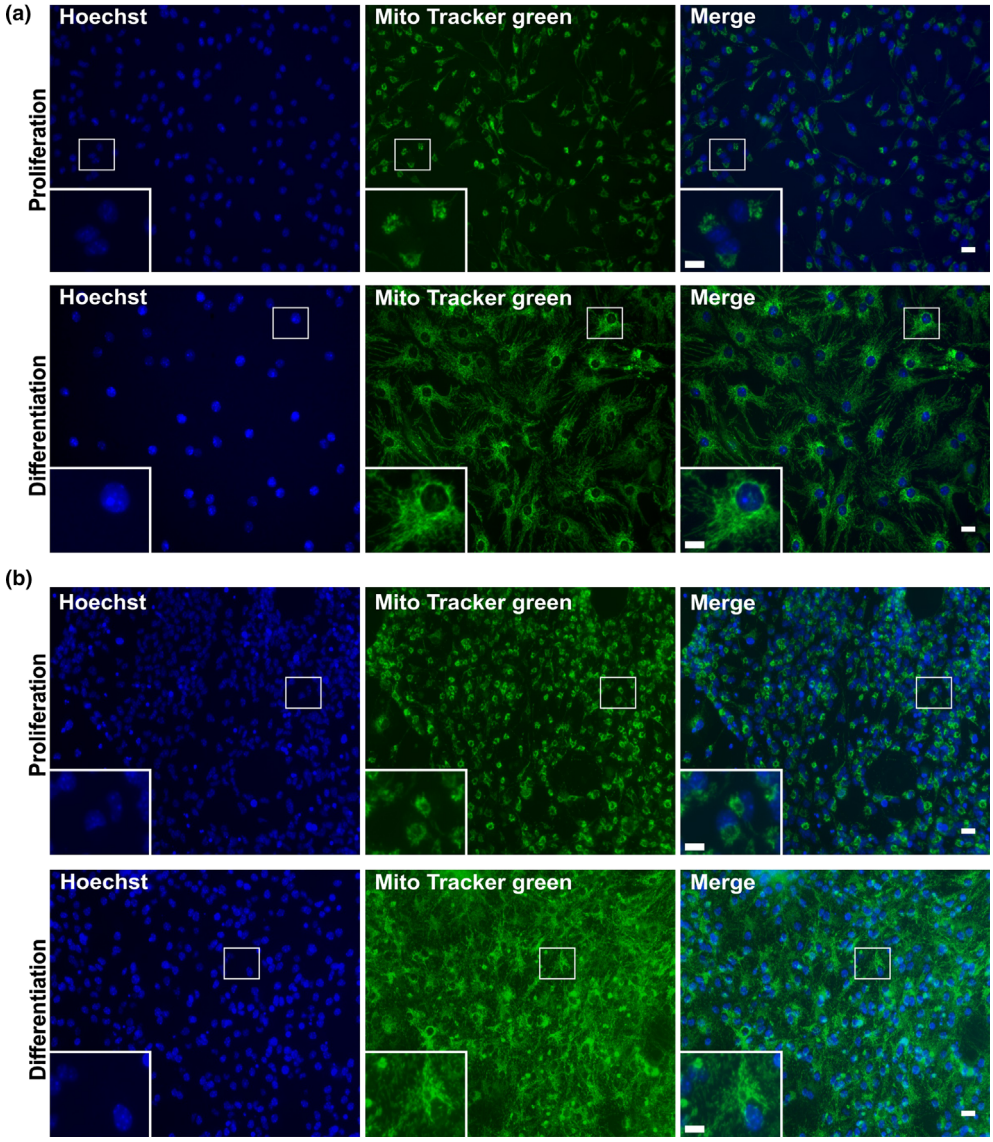

FIGURE 1 Mitochondrial morphology upon differentiation of neural stem cells (NSCs). MitoTracker green staining of CGR8-NS cells (a) and primary NSCs (b) in proliferation and neural differentiation. Proliferating cells show mitochondrial distribution around the nucleus, whereas their differentiated derivatives show more evenly distributed mitochondria throughout the cytoplasm. Nuclei were counterstained with Hoechst 33342 and are shown in blue. The bottom left insets display high magnification of the marked areas. Scale bar, 20 μm. Scale bar within magnified images, 10 μm.

When more than two groups were compared, statistical analysis was performed using one-way or two-way analysis of variance, followed by Bonferroni adjusted post-hoc *t*-test to compute the statistical difference between the groups. All data are presented as means ± standard error of the mean; *p* values of <.05 were considered significant.

3 | RESULTS

3.1 | Mitochondrial distribution upon differentiation of NSCs

To investigate mitochondrial function during gliogenesis in NSCs, we initially used the CGR8-NS cell line generated by Conti and colleagues by using a lineage selection technique to produce homogeneous and pure NSC cultures (Conti et al., 2005; Li et al., 1998). CGR8-NS cells have characteristics similar to those of radial glial cells, but they differentiated solely into GFAP$^+$ astroglial cells. Consistently, we could not detect any signal for the neuron marker β-tubulin III after differentiation. The advantage of this cell line is its homogeneity and easy availability for biochemical analysis. In addition, we used primary fetal NSCs directly isolated from mouse forebrain tissue with glial and neural differentiation capacity (Geschwind et al., 2001). CGR8-NS cells and NSCs were stained with MitoTracker green dye, which accumulates in the matrix of metabolically active mitochondria (Figure 1). Proliferating CGR8-NS cells showed a clustered perinuclear arrangement of mitochondria, whereas a scattered cytoplasmic distribution was observed in their glial progeny (Figure 1a). Similar morphological changes were observed in primary NSCs upon neuroglial differentiation (Figure 1b).

3.2 | Mitochondrial biogenesis upon differentiation of NSCs

The mtDNA copy number varies among different cell types and tissues (Mao & Holt, 2009) and is directly related to mitochondrial

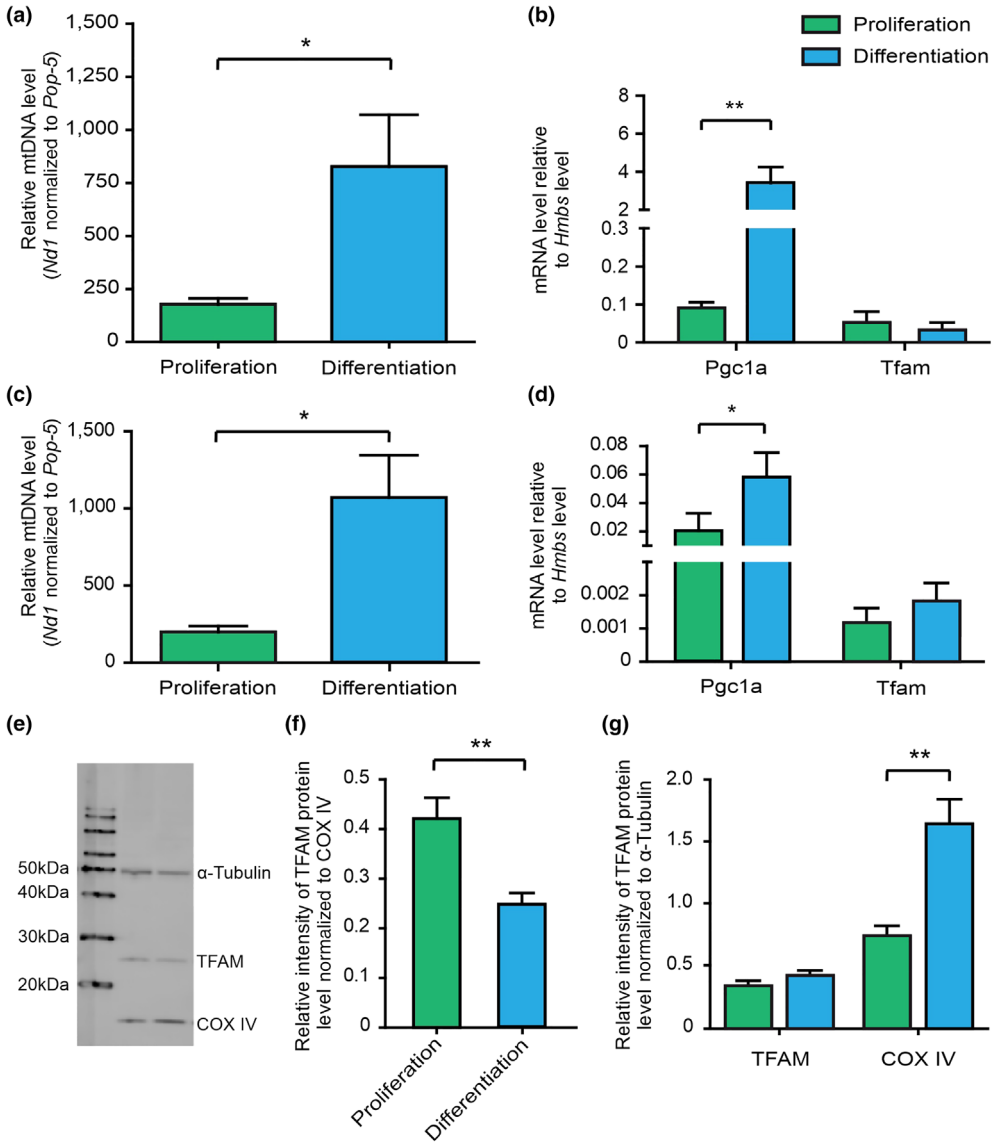

FIGURE 2 Mitochondrial biogenesis upon differentiation of neural stem cell (NSC) types. (a, c) Relative mtDNA level (mtDNA encoded *Nd1* normalized to *Pop5* as a nuclear encoded gene) of CGR8-NS cells (a) and primary NSCs (c). mtDNA copy number was measured in proliferating cells (2 days after splitting for CGR8-NS cells, 7 days after isolation for primary NSCs) and in cells differentiated for 7 days using quantitative RT-PCR. (b, d) mRNA expression levels of the mitochondrial biogenesis-associated genes *Pgc1α* and *Tfam* in proliferating and differentiated CGR8-NS cells (b) and primary NSCs (d). Housekeeping gene *Hmbs* was used as reference. (e–g) Western blot analysis of mitochondrial transcription factor A (TFAM) expression in mitochondrial fraction of proliferating and differentiated CGR8-NS cells. TFAM protein was first normalized to COX IV as a commonly used mitochondrial loading control (f) showing a decrease in TFAM protein level. By using α-Tubulin (50 kDa) as a loading control independent of mitochondrial protein expression, TFAM expression was unchanged and COX IV protein expression was increased upon differentiation (g). The values represent means ± SEM from at least three to six independent experiments. * denotes $p < .05$, ** denotes $p < .01$ (two-sided unpaired *t*-test).

function; i.e. cells with higher energy demand have higher mtDNA copy numbers. To determine mtDNA copy number, the mitochondrial gene encoding for one of the subunits of complex I, namely NADH dehydrogenase 1 (Nd1), was amplified and its content was normalized to the content of the nuclear encoded gene encoding for nuclear processing of precursor 5 (Pop5, a subunit of RNase MRP). Nd1 is located in the minor arc of the mitochondrial genome, an area which is known to be unaffected by specific mtDNA deletion as occurring in the major arc (Belmonte et al., 2016; Chen et al., 2011). The relative expression of the Nd1 gene is therefore a suitable and common measure of the relative copy number of mtDNA (Augustyniak et al., 2017; Dickinson et al., 2013; Dolle et al., 2016). In differentiated cells a nearly, five- to seven-fold increase was observed in mtDNA copy number compared with proliferating cells in both NSC types (Figure 2a, c). To explore mitochondrial biogenesis, mRNA expression levels of two major regulators associated with mitochondrial biogenesis, Pgc1α and Tfam, were examined in both NSC types: higher expression levels

of Pgc1α were observed in differentiated cells compared with proliferating cells, but expression levels of Tfam were similar in both conditions (Figure 2b, d).

We next performed Western blot analysis to confirm that there is no change of TFAM expression upon neural differentiation of NSCs (Figure 2e–g). Normalization of TFAM protein levels to the established mitochondrial loading control COX IV (Yu et al., 2007) showed a decrease of TFAM protein level (Figure 2e, f). As COX IV seemed to be upregulated upon differentiation, we additionally used α-tubulin as a loading control that binds to mitochondrial membranes during isolation of mitochondria (Bernier-Valentin et al., 1983; Liang et al., 2006; Yang et al., 2018), thus being independent of mitochondrial protein expression. Normalization to α-tubulin revealed that TFAM expression was unchanged, whereas COX IV protein expression was increased upon differentiation (Figure 2g). The upregulation of COX IV expression upon differentiation further confirmed that neural differentiation involves activation of mitochondrial function, in this case aerobic energy metabolism.

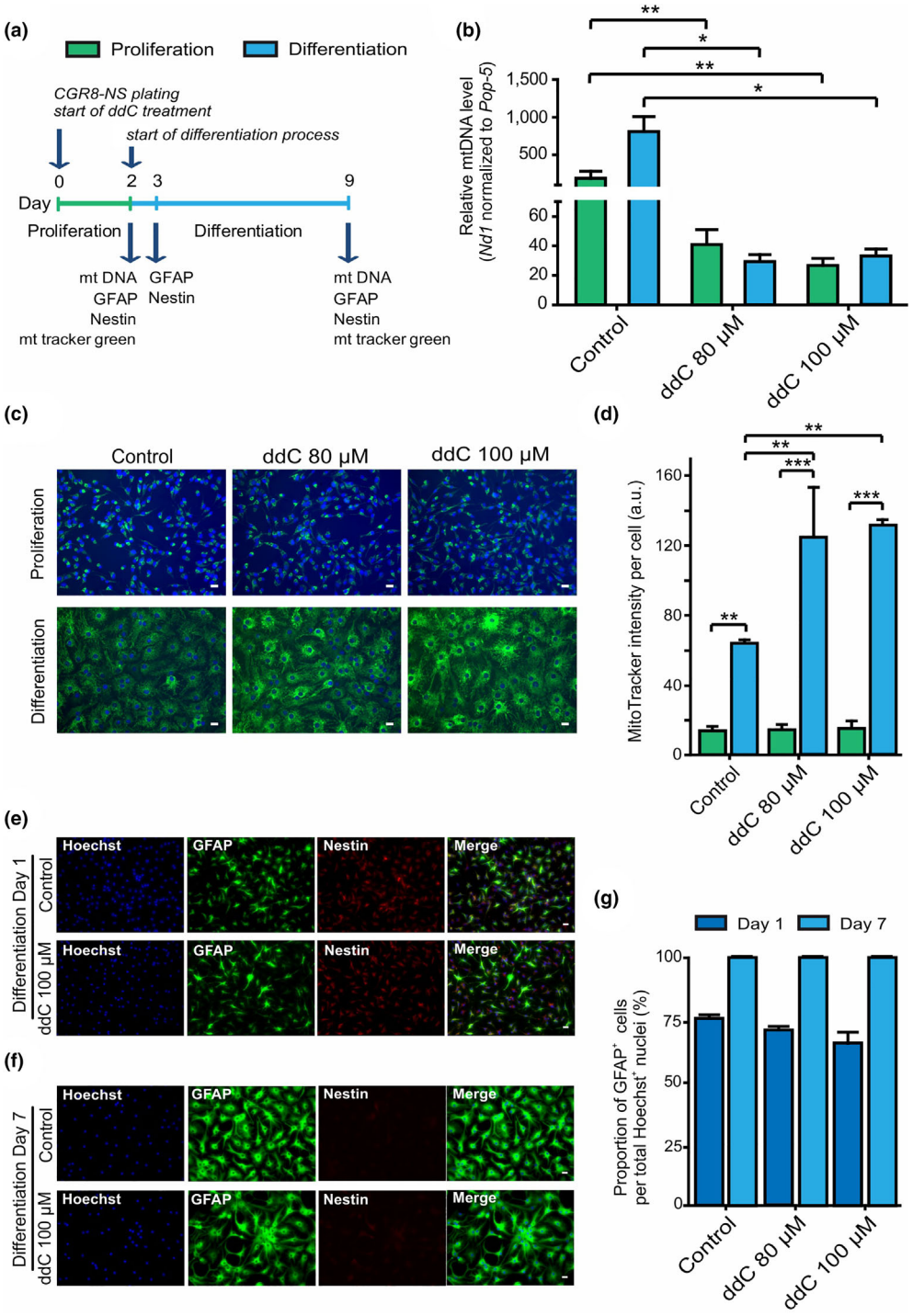

FIGURE 3 Legend on next page.

3.3 | Depletion of mtDNA by ethidium bromide results in early NSC death

The observed increase in mitochondrial biomass upon neural differentiation of NSCs prompted us to investigate the effects of mtDNA on differentiation capacity of NSCs. We tried to generate CGR8-NS cells lacking mtDNA (ρ° cells) using long-term treatment with ethidium bromide (EthBr) at a concentration range from 0.0625 to 0.5 μg/mL, which is known to work in human cells and mouse fibroblasts (Hayashi et al., 1990; King & Attardi, 1996). Unfortunately, no viable mouse ρ° NSCs could be generated using this approach because of early cell death. This is in accordance with the studies by Fike and colleagues for murine adult NSCs (Fike et al., 2009) and described in Hashiguchi and Zhang-Akiyama (2009). Possibly, long-term treatment with EthBr exhibits a higher cytotoxicity in NSCs compared with other somatic cells such as fibroblasts (King & Attardi, 1996).

3.4 | Effects of inhibition of mtDNA replication by ddC in NSCs

As outlined above, there are two key factors that directly regulate the mtDNA replication, namely TFAM and the mtDNA polymerase-γ (POLG) (Clayton, 1982; Clayton, 1992). As no changes were observed in TFAM expression level upon differentiation, we next focused on the role of POLG by inhibiting its activity using ddC. NSCs were treated with ddC during proliferation and differentiation starting from the first day (CGR8-NS) or starting on day 5 after NSC preparation (primary fetal NSCs) until the end of the differentiation period (Figures 3 and 4). After 9 days of treatment with ddC, the mtDNA amount was decreased leaving only a residual amount of mtDNA (Figures 3b and 4b).

To address changes of the mitochondrial mass, we next analyzed MitoTracker during proliferation and differentiation in presence and absence of ddC (Figure 3c, d). Quantification of the MitoTracker signal per cell revealed a dramatic increase of MitoTracker in differentiated NSCs compared with proliferating NSCs, which is in concordance with their increase in mtDNA (Figure 3d). Interestingly, ddC treatment further increases the MitoTracker signal in differentiated cells but has no effects in proliferating cells.

The reduction of mtDNA replication, and hence of mtDNA content, during proliferation neither affected the total number of cells nor induced the formation of condensed cell nuclei (Figures S1 and S2), implicating no effects of mtDNA reduction on NSC proliferation. However, total cell counts per image revealed that ddC treatment accelerates glial fate determination of CGR8-NS, which either differentiate into astrocytes or die (Figures S1 and S3) (Conti et al., 2005). In contrast, total cell counts per image revealed no changes in primary NSCs (Figure S4). Consistently, immunoreaction analysis revealed neither a change in the morphology nor a change in the number of Nestin$^+$ NSCs upon ddC treatment (Figures S1 and S2). This is in line with previous reports showing that stem cells depend on glycolysis instead of oxidative phosphorylation for their energy supply (Braunschweig et al., 2022; Iwata & Vanderhaeghen, 2021). Consistently, intracellular ATP levels and ATP:ADP ratios were not affected by ddC treatment during proliferation (Figure 5a,b) and the remaining mtDNA content seems therefore to be sufficient to maintain NSC proliferation (Khacho et al., 2017; Van Den Ameele & Brand, 2019).

3.5 | Effects of inhibition of mtDNA replication on NSC differentiation

To investigate whether depletion of the mtDNA level interferes with glial differentiation capacity, CGR8-NS cells were stained for the glial cell marker GFAP during proliferation as well as after differentiation (1 and 7 days after initiation of differentiation; Figure 3e–g). As known from previous studies (Conti et al., 2005; Li et al., 1998), CGR8-NS cells did not express GFAP during proliferation, but switched to GFAP$^+$ glial cells in large numbers after differentiation

FIGURE 3 Influence of mtDNA depletion on glial differentiation capacity of the CGR8-NS cells. (a) Schematic representation of 2′-3′-dideoxycytidine (ddC) treatment paradigm. (b) Effects of ddC treatment on mtDNA copy numbers measured in proliferating cells (after 2 days) and cells differentiated for 7 days using quantitative RT-PCR under control and ddC treatment condition. Two-way ANOVA with *post-hoc t*-test and Bonferroni adjustment with developmental stage (proliferation/differentiation) and ddC treatment as fixed factors revealed that developmental stage and treatment have a significant interaction effect on mtDNA levels ($p = .039$, F-value = 3.6) and significant differences among developmental stage ($p = .042$, F-value = 3.0) and treatments ($p = .002$, F-value = 7.7). (c) MitoTracker immunoreactivity in proliferating and differentiated CGR8-NS cells after treatment with 80 μM or 100 μM ddC or no treatment. Scale bar, 20 μm. (d) Quantification of summed MitoTracker intensity per cell in proliferating and differentiated CGR8-NS cells after treatment with 80 or 100 μM ddC or no treatment. Two-way ANOVA with *post-hoc t*-test and Bonferroni adjustment with developmental stage (proliferation/differentiation) and ddC treatment as fixed factors revealed that developmental stage and treatment have a significant interaction effect ($p = .008$, F-value = 6.8) as well as significant differences among treatments ($p = .015$, F-value = 5.6) and developmental stage ($p < .001$, F-value = 129.5). (e, f) CGR8-NS cells at differentiation days 1 and 7 upon ddC treatment showing strong immunoreactivity against GFAP. Nuclear staining is shown in blue (Hoechst 33342). Scale bar, 20 μm. (g) Quantification of GFAP$^+$ cells (percentage of total cell number) at differentiation day 1 and day 7 under control and treatment condition. Two-way ANOVA with *post-hoc t*-test and Bonferroni adjustment with developmental stage (proliferation/differentiation) and ddC treatment as fixed factors revealed that developmental stage and treatment have no significant interaction effect on GFAP$^+$ cell counts ($p = .062$, F-value = 3.3) and no significant differences among treatments ($p = .066$, F-value = 3.2), but significant differences between developmental stage ($p < .001$, F-value = 190.6). Data are presented as means ± SEM of at least three independent experiments. Bonferroni adjusted two-sided *post-hoc* t-test *p*-values with * denoting $p < .05$, ** denoting $p < .01$ and *** denoting $p < .001$.

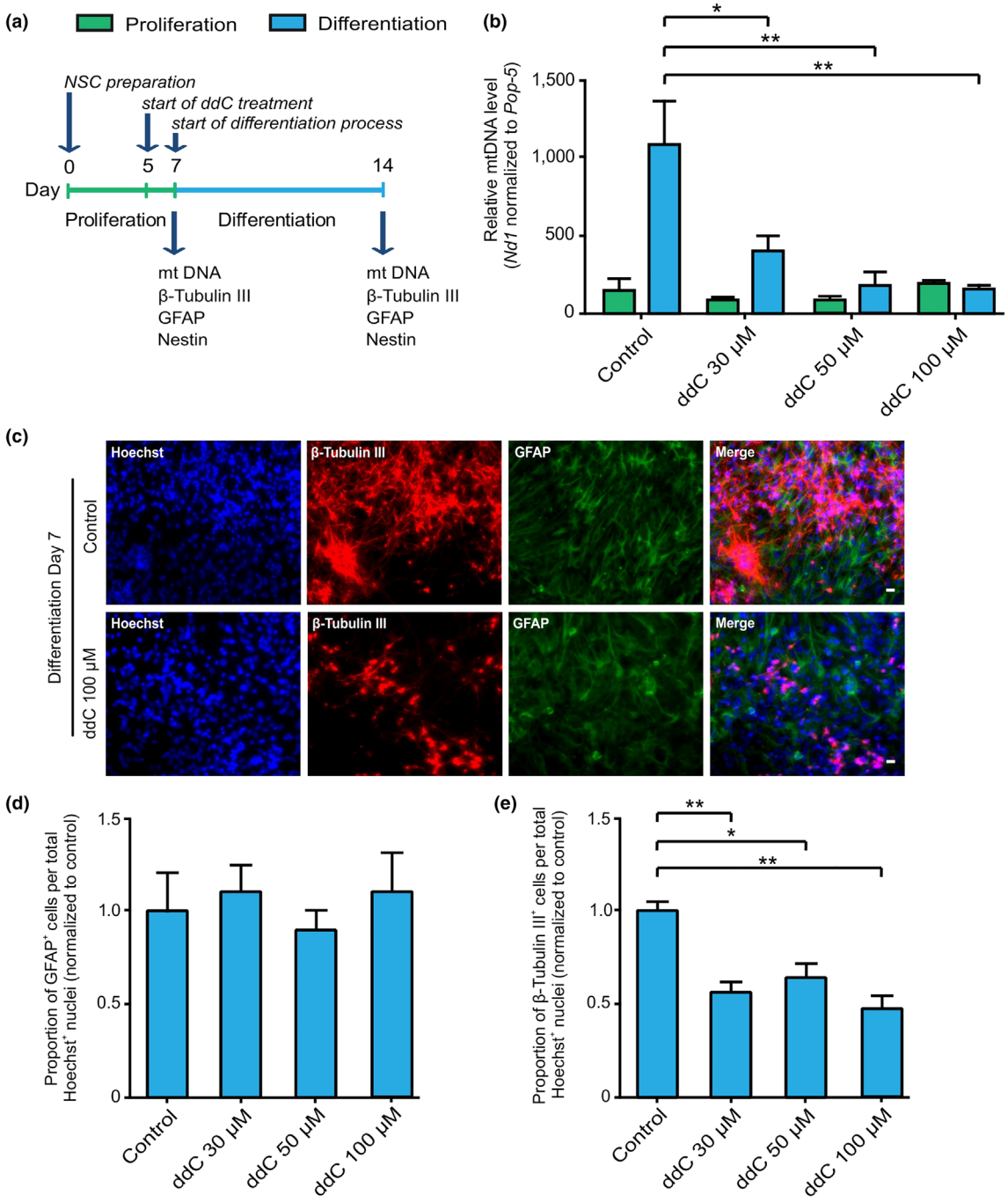

FIGURE 4 Effects of mtDNA depletion on primary forebrain derived neural stem cells (NSCs). (a) Schematic representation of 2′-3′-dideoxycytidine (ddC) treatment paradigm. (b) Effects of ddC treatment on the mtDNA copy number in E14 forebrain-derived NSCs. Two-way ANOVA with *post-hoc t*-test and Bonferroni adjustment with developmental stage (proliferation/differentiation) and ddC treatment as fixed factors revealed that developmental stage and treatment have a significant interaction effect on mtDNA levels ($p = .002$, F-value = 7.2) and significant differences among developmental stage ($p < .001$, F-value = 19.8) and treatments ($p = .001$, F-value = 8.1). (c) Immunoreactivity against GFAP (astroglia) and β-Tubulin III (neurons) after 7 days of differentiation under control and ddC (100 µM) treatment condition. ddC treatment led to less β-Tubulin III$^+$ cells whose neurites appear shorter while GFAP expression was not affected. The nuclei were counterstained with Hoechst 33342. Scale bar, 20 µm. (d) Quantification of GFAP$^+$ cells at differentiation day 7 under control and treatment conditions. One-way ANOVA revealed no significant changes in the number of GFAP$^+$ cells upon treatment ($p = .670$; F = 0.53). (e) Quantification of β-Tubulin III$^+$ neurons at differentiation day 7 under control and treatment conditions. One-way ANOVA revealed significant differences in the number of β-III-Tubulin$^+$ cells upon treatment ($p = .001$; F = 17.15). Data are presented as means ± SEM of at least three independent experiments. Bonferroni adjusted two-sided *post-hoc t*-test *p*-values with * denoting $p < .05$, ** denoting $p < .01$, and *** denoting $p < .001$.

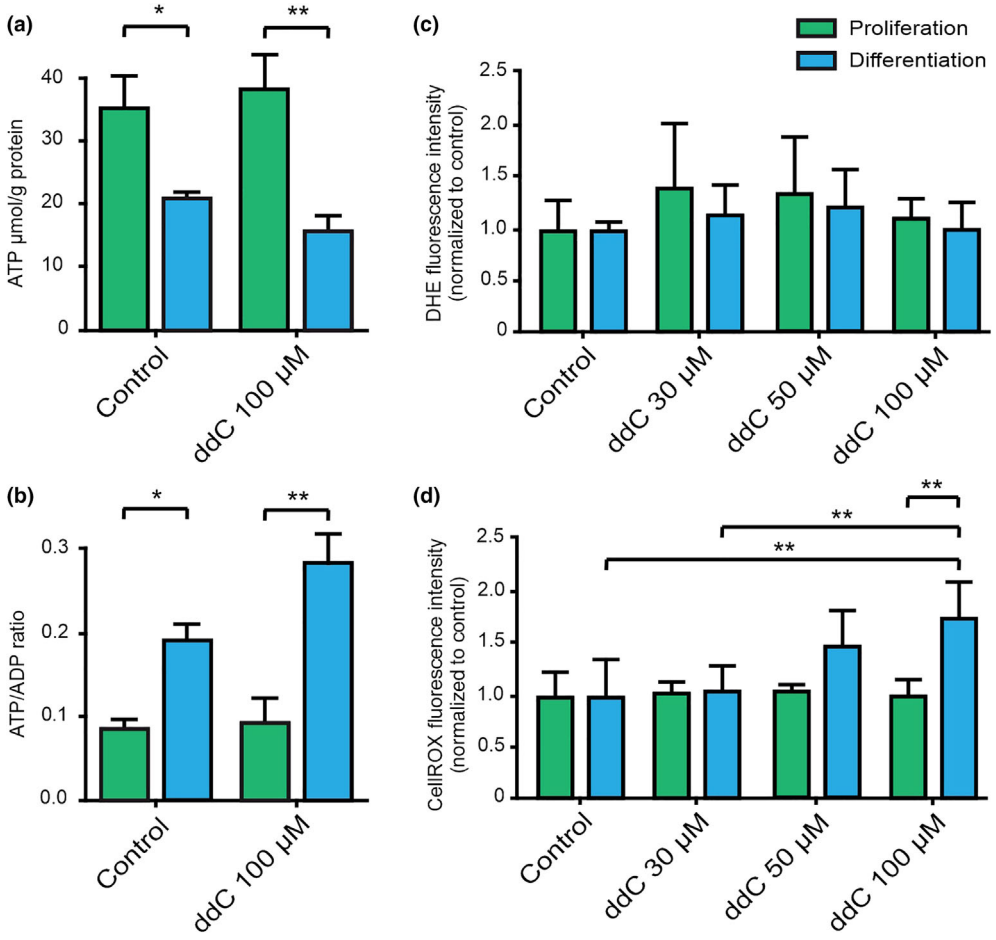

FIGURE 5 Effects of mtDNA depletion on energy metabolism of primary isolated neural stem cells (NSCs) during differentiation. (a) Intracellular ATP level in proliferation and differentiation under control and 2′-3′-dideoxycytidine (ddC) treatment conditions. Two-way ANOVA with *post-hoc t*-test and Bonferroni adjustment with developmental stage (proliferation/differentiation) and ddC treatment as fixed factors revealed that developmental stage and treatment have no significant interaction effect on ATP levels ($p = .283$, F-value = 1.3) and no significant differences among treatments ($p = .823$, F-value = 0.1), but significant differences between developmental stages ($p = .001$, F-value = 23.7). (b) ATP:ADP ratio under proliferation and differentiation condition in control and ddC treatment condition. Two-way ANOVA with *post-hoc t*-test and Bonferroni adjustment with developmental stage (proliferation/differentiation) and ddC treatment as fixed factors revealed that developmental stage and treatment have no significant interaction effect on ATP:ADP ratio ($p = .583$, F-value = 0.33) and no significant differences among treatments ($p = .746$, F-value = 0.11), but significant differences between developmental stages ($p = .003$, F-value = 18.34). (c, d) Effects of ddC treatment on cellular ROS as measured by dihydroethidium (DHE) (c) and CellROX® staining (d). DHE and CellROX® fluorescence was measured in proliferating (2 days) and differentiated (7 days) cells under control and ddC treatment conditions. Two-way ANOVA with *post-hoc t*-test and Bonferroni adjustment with developmental stage (proliferation/differentiation) and ddC treatment as fixed factors revealed for DHE staining that developmental stage and treatment have no significant interaction effect on DHE fluorescence intensity ($p = .708$, F-value = 0.5) and no significant differences among developmental stage ($p = .087$, F-value = 3.2) and treatments ($p = .253$, F-value = 1.5), and for CellROX® staining that developmental stage and treatment have no significant interaction effect ($p = .078$, F-value = 2.6) but significant differences among developmental stage ($p = .012$, F-value = 7.3) and treatments ($p = .005$, F-value = 5.6). Data are presented as means ± SEM of at least three independent experiments. Bonferroni adjusted two-sided post hoc *t*-test *p*-values with * denoting $p < .05$, and ** denoting $p < .01$.

(Figure 3G, Figure S1a). Interestingly, the number of GFAP$^+$ astroglial cells after differentiation were not affected by mtDNA depletion (Figure 3g). Of note, most of the CGR8-NS cells were lost through initiation of differentiation, but no condensed nuclei could be observed 7 days after differentiation, which indicates an absence of apoptotic processes due to ddC treatment. The data show that these cells did not lose their ability to differentiate into glia even though the mtDNA level was decreased by ~97%.

We next analyzed the effects of mtDNA depletion on the neural differentiation capacity of primary NSCs that allowed us to investigate glial and neuronal specifications in the same culture (Figure 4a). Treatment with ddC significantly reduced the mtDNA level in differentiated derivatives down to the levels of undifferentiated NSCs (Figure 4b). After differentiation, no significant changes were observed in the number of GFAP$^+$ cells when comparing ddC treatment conditions to control condition (Figure 4c, d). After 7 days of differentiation,

however, immunocytochemical analysis revealed morphological changes with shorter neurites and markedly reduced numbers of β-tubulin III$^+$ neurons in ddC-treated cultures in comparison to control conditions (Figure 4c, d). Of note, ddC treatment did not influence cell survival during proliferation and differentiation (Figure S2c).

To check whether these effects on mtDNA depletion are related to changes in cellular energy state, HPLC-based analyses were performed in NSCs and their differentiated derivatives that were treated with the highest ddC concentration used (100 μM). Neither intracellular ATP levels nor ATP:ADP ratios were changed upon ddC treatment when compared with control samples (Figure 5a,b). We next tested the effects of ddC treatment on cellular ROS using DHE and CellROX® staining in proliferating and differentiated cells (Figure 5c,d). Treatment with up to 100 μM ddC did not significantly change cellular ROS levels of proliferating or differentiated cells as measured by DHE, which is associated with hyperoxide ROS (Figure 5c). The CellROX® detection assay, which is more sensitive to various ROS, revealed an increase in cellular ROS in the differentiated cell state incubated with ddC concentrations of 50 μM and higher (Figure 5d). In conclusion, ddC-induced mtDNA depletion resulted in a reduced number of β-tubulin III$^+$ cells in differentiated primary NSCs while neither affecting the amount of GFAP$^+$ cells nor proliferation.

4 | DISCUSSION

The present study demonstrates the pivotal involvement of mtDNA replication in the differentiation potential of NSCs into nerve cells, but not glial cells. Inhibition of mtDNA replication by ddC leads to reduction of cellular mtDNA content, which consequently impairs the ability of NSCs to adapt their mtDNA levels to their differentiated state. This specific mitochondrial defect efficiently blocks early neuronal, but not glial, differentiation of NSCs. As ATP content and the ATP:ADP ratio as a sensitive measure of cellular energy state (Metallo & Vander Heiden, 2013; Yuan et al., 2013) as well as cellular ROS content remain largely unchanged in ddC-treated cells, the effects of mtDNA depletion on neurogenesis are most likely not mediated by changes in cellular energy metabolism or ROS production.

Studies on mitochondrial morphology in both NSC types, such as ESC-derived CGR8-NS cells and primary NSCs isolated from fetal mouse (E14) forebrain, showed a differential mitochondrial pattern in undifferentiated NSCs compared with their differentiated counterparts: a clustered perinuclear arrangement was characteristic for NSCs, whereas a more dispersed and cytoplasmic distribution was typical for differentiated cells, which is in accordance with previous studies (Cho et al., 2006; Lonergan et al., 2006). Indeed, Lonergan and colleagues suggested that mitochondrial properties, such as metabolic activity or subcellular distribution, can be used as markers of stemness or proliferative state (Lonergan et al., 2006) with a perinuclear arrangement of mitochondria being characteristic for stem cells and a more dispersed mitochondrial distribution being characteristic for differentiated cells. The changes in mitochondrial distribution of NSCs undergoing differentiation coincided with a significant increase in mtDNA levels. These findings are in accordance with previous observations showing increased mitochondrial biomass and mtDNA copy number upon differentiation of various stem and cancer cells including NSCs (Cho et al., 2006; Dickinson et al., 2013; Facucho-Oliveira et al., 2007; Lee et al., 2015; St John et al., 2005). Indeed, Augustyniak and co-workers also showed an increase of mitochondrial biomass and mtDNA cellular content during early differentiation of induced pluripotent stem cell-derived NSCs (Augustyniak et al., 2017; Augustyniak et al., 2019). Taken together, these data point to a major role of mitochondrial function, and particularly of mtDNA replication, in NSC differentiation.

We therefore focused on the involvement of mtDNA and its replication in NSC differentiation properties. For this, we aimed to create an NSC line completely devoid of mtDNA (ρ° NSCs) as demonstrated in several other cells types (Desjardins et al., 1985; Desjardins et al., 1986; King & Attardi, 1989; Morais et al., 1980). However, previous studies failed in creating mouse ρ° cell lines when the cells were treated with EthBr (Hashiguchi & Zhang-Akiyama, 2009). In particular, approaches to creating ρ° NSCs failed, because the NSCs died within a short period of time after EthBr treatment (Fike et al., 2009). Consistently, our trials to deplete mtDNA in the CGR8-NS cell line by using EthBr were also unsuccessful. As an alternative approach, we have targeted the POLG, which is—along with TFAM—a major factor that directly controls mtDNA replication (Clayton, 1982; Clayton, 1992). TFAM is a direct regulator of mtDNA replication and transcription as well as of mitochondrial biogenesis (Ekstrand et al., 2004; Montoya et al., 1997; Virbasius & Scarpulla, 1994; Wu et al., 1999). However, we did not observe any changes in TFAM expression on either the mRNA or the protein level. This is in contrast to reports in embryonic and adult hippocampal NSCs with TFAM as a relevant regulator of mtDNA copy number and mitochondrial biogenesis (Beckervordersandforth, 2017; Beckervordersandforth et al., 2017; Uittenbogaard et al., 2018). In agreement with other stem and cancer cell types (Lee et al., 2015), TFAM seems not to be the major factor in mtDNA replication during gliogenesis and, most likely, not during early neurogenesis in fetal NSCs (Dickinson et al., 2013). Nevertheless, TFAM seems to be essential for survival and differentiation of NSCs as TFAM depletion leads to cell cycle arrest as well as impaired neuronal differentiation and maturation (Kuroda et al., 2021; Qi et al., 2022). Surprisingly, Kuroda and colleagues found a severe reduction not only of neuronal but also of glial differentiation. However, they also showed a dramatic reduction of BrdU$^+$ cells showing a general reduction of cell division, which is needed for neuron as well as astrocyte production. In contrast, the specific POLG inhibitor ddC (Chen et al., 1991; Wang et al., 1997) reduced mtDNA copy number during proliferation in the CGR8-NS cell line and completely blocked the upregulation of mtDNA during the differentiation process in both NSC types without major morphological changes or increased cell death. Obviously, the regulation of mtDNA replication is highly specific for the various stem cell types, including various NSC subtypes, and might additionally depend on the experimental conditions.

Inhibition of mtDNA replication did not influence cell survival or stem cell morphology of both NSC types in our experimental

conditions, but selectively reduced neurogenesis without affecting gliogenesis from NSCs even after treatment with low concentrations of ddC (30 μM). Despite it having been shown that ddC is able to cause neuron-specific damage (Dalakas et al., 2001; Liu et al., 2014), in our conditions, the ddC treatment did not influence cell survival or stem cell morphology of both NSC types, which suggests a specific suppression of neuronal fate determination rather than neuron-specific cell death. On the other hand, gliogenesis was neither affected in CGR8-NS cells nor in primary NSCs, which is in line with data from Chen and colleagues who used iPSCs from patients with *Polg* mutations (Chen et al., 2022). In accordance, astrocytes are reported to be generally more dependent on glycolysis instead of mitochondrial metabolism, additionally explaining the unaffected gliogenesis (reviewed in Belanger et al., 2011, Bonvento & Bolanos, 2021). A recent study using patient-derived iPSCs bearing a *Polg* mutation for 3D brain organoid could show further that POLG not only specifically reduces neurogenesis, but also shifts the specific neuronal differentiation from dopaminergic neurons to GABAergic and glutaminergic neurons (Chen et al., 2024). Patient-derived iPSCs bearing a *Polg* mutation themselves and astrocytes cultivated from them seem to be not as much affected by the mutation as the derived NSCs (Hong et al., 2023; Liang et al., 2020). Moreover, β-tubulin III^{+} neurons showed clear morphological changes with shorter neurite formation in comparison to neurons grown in control conditions, indicating a more immature neuronal differentiation state. The phenomenon of shorter neurites was also described by Verma and colleagues who investigated neurons derived from iPSCs harboring *Polg* mutations (Verma et al., 2023). Wang and co-workers observed similar effects on neural differentiation of primary NSCs by another approach to impair mtDNA function. They produced mtDNA damage by knocking out the enzyme 8-oxoguanine DNA glycosylase as an essential enzyme for mtDNA repair (Wang et al., 2011). The authors claim that the activation of astrogenesis-promoting Sirt1 by oxidative stress is responsible for this shift in NSC differentiation fate. Beckervordersandforth and co-workers also reported that in vivo genetic ablation of TFAM inhibits adult hippocampal neurogenesis (Beckervordersandforth et al., 2017). Contributing to this, mtDNA depletion achieved by TFAM knock-down massively decreased neuronal differentiation (Kuroda et al., 2021; Qi et al., 2022). However, gliogenesis was also affected by TFAM knock-down whereas the POLG-induced mtDNA depletion solely affected neurogenesis but not gliogenesis.

It is well known that the increase in mtDNA content and mitochondrial biomass upon the differentiation process of stem cells into their differentiated derivatives—as observed in our fetal NSC model—is associated with a switch from anaerobic energy production to oxidative phosphorylation (Agathocleous et al., 2012; Homem et al., 2014; Wanet et al., 2015; Xavier et al., 2016; Zheng et al., 2016). Unexpectedly, mtDNA depletion by ddC did not alter intracellular ATP levels and ATP:ADP ratios, reflecting cellular energy metabolism in NSCs after 7 days of differentiation (9 days of treatment). However, similar data were obtained for human iPSCs: short-term mtDNA depletion (5 days) did not affect ATP production, and only long-term (10 days) led to a reduction of ATP (Qi et al., 2022). Moreover, severe changes in energy metabolism as well as ROS production have been shown in iPSC-derived NSCs bearing a *Polg* mutation that were passaged several times (Hong et al., 2023; Liang et al., 2020). This probably reflects a very long-term mtDNA depletion, which further demonstrates that the duration of POLG-mediated mtDNA depletion plays an important role for its consequences on energy and ROS metabolism. The reasons for this lack of short-term mtDNA depletion effects remain enigmatic but might include the stability of mitochondrial enzyme complexes of the oxidative phosphorylation system during the rather short experimental time period and/or their re-arrangement in super-complexes as observed in other stem cell systems upon differentiation (Hofmann et al., 2012). As ddC treatment is not reported to affect mtDNA transcription (Kuthethur et al., 2022), increased expression of the remaining mtDNA might also be involved in compensating the effects of mtDNA depletion in our cell lines. Alternatively, our approach to target the mtDNA using POLG inhibition may lead to less energy consumption, as in the case of previously used methods largely inducing mtDNA damage and subsequently energy-dependent DNA repair mechanisms. However, alterations of cellular energy metabolism, at least ATP metabolism, are not responsible for the effects of mtDNA depletion on early NSC differentiation.

Another possible mechanism mediating the actions of mtDNA depletion on NSC differentiation might involve mitochondrial generation of ROS, which have recently been found to regulate NSC proliferation, lineage commitment, and differentiation (Beckervordersandforth, 2017; Forsberg et al., 2013; Kahroba et al., 2020; Khacho et al., 2016; McBride et al., 2006; Oswald et al., 2018). In our experimental setup, mtDNA depletion provoked an increase in cellular ROS content only at high concentrations of ddC when measured by the CellROX technique, but not via DHE measurement. This difference is potentially caused by the specificity of DHE for hyperoxide ROS (Chen et al., 2009). As even lower concentrations of ddC reduce neurogenesis, it is highly unlikely that the effects of mtDNA depletion on neurogenesis in primary NSCs are mediated through changes in cellular redox state. Despite their mtDNA depletion being achieved by TFAM knock-down, Qi and colleagues observed something similar: while short-term (5 days) mtDNA depletion did not change ATP production, a long-term mtDNA depletion massively reduced ATP production most likely caused by destroyed mitochondria (Qi et al., 2022). In contrast, this did not reflect their redox state, as both long-term and short-term cultivated cells showed dramatically reduced ROS levels when analyzed by CellROX as well as by MitoSox (Kuroda et al., 2021, Qi et al., 2022). However, an increase of ROS levels (analyzed by DCFDA) has been shown for iPSC-derived NSCs bearing a *Polg* mutation and passaged several times showing further differences of TFAM- or POLG-mediated mtDNA depletion (Liang et al., 2020). Growing evidence indicates that mitochondria are an integral part of multiple cell signaling cascades with Ca^{2+} signaling, various GTPases, kinases, and phosphatases being involved in bi-directional communication between the mitochondrion and other cell components including the nucleus (McBride et al., 2006). Future studies are needed to determine the specific cascade of this mitochondrion–cytoplasm–nucleus communication regulating cell fate decisions in NSCs.

In ancillary analyses, we observed not only an increase of the mitochondrial biomass upon differentiation of NSCs but also by inhibition mtDNA replication using ddC in differentiated NSCs. This increase in biomass might reflect the interplay between reduced mtDNA replication and mitochondrial morphology and dynamics (Chen et al., 2010; Silva Ramos et al., 2019; Viscomi & Zeviani, 2017). Interestingly, it was shown in the 1990s that mitochondria contain about 50–100 copies of mtDNA that enable them to divide without further mtDNA replication until one to five copies of mtDNA remain (Kuroiwa et al., 1994). In human cells the number of mtDNA copies that are organized in nucleoids reaches several hundreds and multiple copies of mtDNA can be allocated in a single mitochondrion (Kukat et al., 2011; Legros et al., 2004; Satoh & Kuroiwa, 1991). However, the connection of mtDNA copy number per mitochondrion with mitochondrial biomass is still very poorly understood, potentially because of high mitochondrial dynamics. Physiologically, mitochondria are elongated in NSCs, fragmented in NPCs, and again elongated in neurons (reviewed in Coelho et al. (2022). Indeed, mitochondrial fusion is not only linked to mtDNA replication, but also directs NSCs to self-replication instead of neuroglial differentiation, presumably by modifying ROS signaling (Iwata et al., 2020; Khacho et al., 2016). Contributing to this, mitochondrial fusion and fission appear to be generally important for stem cell fate and neuronal maturation, as well as neuronal survival (Fang et al., 2016; Jahani-Asl et al., 2011; Kochan et al., 2024). The research groups investigated various neuronal stem cell types by knocking-down or overexpressing mitofusin (MFN/*Mfn*) genes. A reduction of MFN prevented the fusion of mitochondria, which subsequently impaired neuronal differentiation and maturation, whereas, vice versa, overexpression of MFN2 led to increased neurogenesis and survival. However, while the mechanism of fusion and fission of mitochondria affecting neurogenesis fits very well with our model, MFN/*Mfn* genes are coded chromosomally and therefore are not directly affected by mtDNA depletion. Not much is known about the effects of POLG or mtDNA depletion on fusion/fission of mitochondria. That POLG can affect fusion/fission of mitochondria has been shown in zebrafish or smooth muscle cells, but—to the best of our knowledge—not yet in NSCs (Branas Casas et al., 2024; Silva Ramos et al., 2019; Zhu et al., 2023). Unfortunately, our data about mitochondrial biomass are limited to CGR8-NS cells, as it was impossible to distinguish the MitoTracker signal between individual cells in primary NSCs due to their strong arborization and overlapping of the cells. Nevertheless, our data show that future studies are warranted to investigate the interplay between mtDNA content and the mitochondrial fusion–fission balance as a factor involved in neurogenesis in fetal NSCs.

Although, it is in principle possible that ddC might provoke as yet unknown cellular effects that inhibit neurogenesis, ddC is reported to be highly specific for inhibiting mitochondrial POLG activity through its phosphorylated metabolite ddC-triphosphate (ddCTP) in mammalian cells (Wang et al., 1997). This view is supported by the fact that effects of ddC are only observed in cells that are undergoing mtDNA replication. Although actions of POLG independent from mtDNA replication have not yet been described, such actions with mtDNA depletion being only a bystander effect might putatively also explain the observed effects. Dissecting the molecular mechanisms underlying the effects of POLG inhibition on neurogenesis, however, clearly needs further investigations. The other known effect of ddC, namely the therapeutically used action on reverse transcriptase activity to treat retroviral infection (Clayton, 1982), does not play a role in our cell system.

In conclusion, mtDNA replication is essential for early neurogenesis events, but not for gliogenesis, in fetal NSCs. Although the underlying mechanisms are still unclear, they are most likely not mediated through alterations in cellular energy metabolism or ROS production. It will be interesting to dissect the cellular signaling pathways and/or metabolic circuits that are enabled by mtDNA-dependent mitochondrial activity in early neurogenic differentiation of NSCs.

AUTHOR CONTRIBUTIONS

M.W.-M.: collection and/or assembly of data, data analysis and interpretation, manuscript drafting, final approval of manuscript. M.M. and J.P.: collection and/or assembly of data, data analysis, final approval of manuscript. F.M.: collection and/or assembly of data, data analysis and interpretation, revision and final approval of manuscript. G.R. and A.D.: data analysis and interpretation, final approval of manuscript. A.H.: conception and design, financial support, data analysis and interpretation, final approval of manuscript. A.S.: conception and design, financial support, assembly of data, data analysis and interpretation, manuscript writing, final approval of manuscript.

ACKNOWLEDGMENTS

We thank Prof. Dr. Wieland Huttner (MPI-CBG, Dresden, Germany) for providing the CGR8-NS cell line; Andreas Hoffmann, Lisa Wagenführ, and Lena Braunschweig for fruitful discussions; and Sylvia Kanzler and Connie May for excellent technical assistance.

FUNDING INFORMATION

This work was supported by the Center for Regenerative Therapies Dresden (CRTD), the Medical Faculty Carl Gustav Carus research funds and the Advocacy for Neuroacanthocytosis Patients, UK. A.H. is supported by the Hermann und Lilly Schilling-Stiftung für medizinische Forschung im Stifterverband.

CONFLICT OF INTEREST STATEMENT

The authors report no conflicts of interest.

DATA AVAILABILITY STATEMENT

The data that support the findings of this study are available on reasonable request from the corresponding author.

ORCID

Franz Markert https://orcid.org/0000-0001-6502-2567

REFERENCES

Agathocleous, M., Love, N. K., Randlett, O., Harris, J. J., Liu, J., Murray, A. J., & Harris, W. A. (2012). Metabolic differentiation in the embryonic retina. *Nature Cell Biology*, *14*, 859–864.

Anderson, S., Bankier, A. T., Barrell, B. G., de Bruijn, M. H. L., Coulson, A. R., Drouin, J., Eperon, I. C., Nierlich, D. P., Roe, B. A., Sanger, F., Schreier, P. H., Smith, A. J. H., Staden, R., & Young, I. G. (1981). Sequence and organization of the human mitochondrial genome. *Nature*, *290*, 457–465.

Attardi, G. (1985). Animal mitochondrial DNA: An extreme example of genetic economy. *International Review of Cytology*, *93*, 93–145.

Augustyniak, J., Lenart, J., Gaj, P., Kolanowska, M., Jazdzewski, K., Stepien, P. P., & Buzanska, L. (2019). Bezafibrate upregulates mitochondrial biogenesis and influence neural differentiation of human-induced pluripotent stem cells. *Molecular Neurobiology*, *56*, 4346–4363.

Augustyniak, J., Lenart, J., Zychowicz, M., Stepien, P. P., & Buzanska, L. (2017). Mitochondrial biogenesis and neural differentiation of human iPSC is modulated by idebenone in a developmental stage-dependent manner. *Biogerontology*, *18*, 665–677.

Beckervordersandforth, R. (2017). Mitochondrial metabolism-mediated regulation of adult neurogenesis. *Brain Plasticity*, *3*, 73–87.

Beckervordersandforth, R., Ebert, B., Schaffner, I., Moss, J., Fiebig, C., Shin, J., Moore, D. L., Ghosh, L., Trinchero, M. F., Stockburger, C., Friedland, K., Steib, K., von Wittgenstein, J., Keiner, S., Redecker, C., Hölter, S. M., Xiang, W., Wurst, W., Jagasia, R., … Lie, D. C. (2017). Role of mitochondrial metabolism in the control of early lineage progression and aging phenotypes in adult hippocampal neurogenesis. *Neuron*, *93*, 1518.

Belanger, M., Allaman, I., & Magistretti, P. J. (2011). Brain energy metabolism: Focus on astrocyte-neuron metabolic cooperation. *Cell Metabolism*, *14*, 724–738.

Belmonte, F. R., Martin, J. L., Frescura, K., Damas, J., Pereira, F., Tarnopolsky, M. A., & Kaufman, B. A. (2016). Digital PCR methods improve detection sensitivity and measurement precision of low abundance mtDNA deletions. *Scientific Reports*, *6*, 25186.

Bereiter-Hahn, J., & Voth, M. (1994). Dynamics of mitochondria in living cells: Shape changes, dislocations, fusion, and fission of mitochondria. *Microscopy Research and Technique*, *27*, 198–219.

Bernier-Valentin, F., Aunis, D., & Rousset, B. (1983). Evidence for tubulin-binding sites on cellular membranes: Plasma membranes, mitochondrial membranes, and secretory granule membranes. *The Journal of Cell Biology*, *97*, 209–216.

Bonvento, G., & Bolanos, J. P. (2021). Astrocyte-neuron metabolic cooperation shapes brain activity. *Cell Metabolism*, *33*, 1546–1564.

Branas Casas, R., Zuppardo, A., Risato, G., Dinarello, A., Celeghin, R., Fontana, C., Grelloni, E., Gilea, A. I., Viscomi, C., Rasola, A., Valle, L. D., Lodi, T., Baruffini, E., Facchinello, N., & Tiso, F. A. N. (2024). Zebrafish polg2 knock-out recapitulates human POLG-disorders; implications for drug treatment. *Cell Death & Disease*, *15*, 281.

Braunschweig, L., Lanto, J., Meyer, A. K., Markert, F., & Storch, A. (2022). Serial gene expression profiling of neural stem cells shows transcriptome switch by long-term Physioxia from metabolic adaption to cell signaling profile. *Stem Cells International*, *2022*, 1–15.

Chen, A., Kristiansen, C. K., Hoyland, L. E., Ziegler, M., Wang, J., Sullivan, G. J., Li, X., Bindoff, L. A., & Liang, K. X. (2022). POLG mutations lead to abnormal mitochondrial remodeling during neural differentiation of human pluripotent stem cells via SIRT3/AMPK pathway inhibition. *Cell Cycle*, *21*, 1178–1193.

Chen, A., Yangzom, T., Hong, Y., Lundberg, B. C., Sullivan, G. J., Tzoulis, C., Bindoff, L. A., & Liang, K. X. (2024). Hallmark molecular and pathological features of POLG disease are recapitulated in cerebral organoids. *Adv Sci (Weinh)*, *11*, e2307136.

Chen, C. H., Vazquez-Padua, M., & Cheng, Y. C. (1991). Effect of anti-human immunodeficiency virus nucleoside analogs on mitochondrial DNA and its implication for delayed toxicity. *Molecular Pharmacology*, *39*, 625–628.

Chen, C. T., Shih, Y. R., Kuo, T. K., Lee, O. K., & Wei, Y. H. (2008). Coordinated changes of mitochondrial biogenesis and antioxidant enzymes during osteogenic differentiation of human mesenchymal stem cells. *Stem Cells*, *26*, 960–968.

Chen, H., Vermulst, M., Wang, Y. E., Chomyn, A., Prolla, T. A., McCaffery, J. M., & Chan, D. C. (2010). Mitochondrial fusion is required for mtDNA stability in skeletal muscle and tolerance of mtDNA mutations. *Cell*, *141*, 280–289.

Chen, T., He, J., Huang, Y., & Zhao, W. (2011). The generation of mitochondrial DNA large-scale deletions in human cells. *Journal of Human Genetics*, *56*, 689–694.

Chen, Y., Azad, M. B., & Gibson, S. B. (2009). Superoxide is the major reactive oxygen species regulating autophagy. *Cell Death and Differentiation*, *16*, 1040–1052.

Cho, Y. M., Kwon, S., Pak, Y. K., Seol, H. W., Choi, Y. M., Park, D. J., Park, K. S., & Lee, H. K. (2006). Dynamic changes in mitochondrial biogenesis and antioxidant enzymes during the spontaneous differentiation of human embryonic stem cells. *Biochemical and Biophysical Research Communications*, *348*, 1472–1478.

Chung, S., Dzeja, P. P., Faustino, R. S., Perez-Terzic, C., Behfar, A., & Terzic, A. (2007). Mitochondrial oxidative metabolism is required for the cardiac differentiation of stem cells. *Nature Clinical Practice. Cardiovascular Medicine*, *4*(Suppl 1), S60–S67.

Clayton, D. A. (1982). Replication of animal mitochondrial DNA. *Cell*, *28*, 693–705.

Clayton, D. A. (1992). Transcription and replication of animal mitochondrial DNAs. *International Review of Cytology*, *141*, 217–232.

Coelho, P., Fao, L., Mota, S., & Rego, A. C. (2022). Mitochondrial function and dynamics in neural stem cells and neurogenesis: Implications for neurodegenerative diseases. *Ageing Research Reviews*, *80*, 101667.

Conti, L., Pollard, S. M., Gorba, T., Reitano, E., Toselli, M., Biella, G., Sun, Y., Sanzone, S., Ying, Q. L., Cattaneo, E., & Smith, A. (2005). Niche-independent symmetrical self-renewal of a mammalian tissue stem cell. *PLoS Biology*, *3*, e283.

Dalakas, M. C., Semino-Mora, C., & Leon-Monzon, M. (2001). Mitochondrial alterations with mitochondrial DNA depletion in the nerves of AIDS patients with peripheral neuropathy induced by 2′3′-dideoxycytidine (ddC). *Laboratory Investigation*, *81*, 1537–1544.

Desjardins, P., De Muys, J. M., & Morais, R. (1986). An established avian fibroblast cell line without mitochondrial DNA. *Somatic Cell and Molecular Genetics*, *12*, 133–139.

Desjardins, P., Frost, E., & Morais, R. (1985). Ethidium bromide-induced loss of mitochondrial DNA from primary chicken embryo fibroblasts. *Molecular and Cellular Biology*, *5*, 1163–1169.

Dickinson, A., Yeung, K. Y., Donoghue, J., Baker, M. J., Kelly, R. D. W., McKenzie, M., Johns, T. G., & St. John, J. C. (2013). The regulation of mitochondrial DNA copy number in glioblastoma cells. *Cell Death and Differentiation*, *20*, 1644–1653.

Dolle, C., Flones, I., Nido, G. S., Miletic, H., Osuagwu, N., Kristoffersen, S., Lilleng, P. K., Larsen, J. P., Tysnes, O.-B., Haugarvoll, K., Bindoff, L. A., & Tzoulis, C. (2016). Defective mitochondrial DNA homeostasis in the substantia nigra in Parkinson disease. *Nature Communications*, *7*, 1–11.

Ekstrand, M. I., Falkenberg, M., Rantanen, A., Park, C. B., Gaspari, M., Hultenby, K., Rustin, P., Gustafsson, C. M., & Larsson, N.-G. (2004). Mitochondrial transcription factor a regulates mtDNA copy number in mammals. *Human Molecular Genetics*, *13*, 935–944.

Facucho-Oliveira, J. M., Alderson, J., Spikings, E. C., Egginton, S., & St John, J. C. (2007). Mitochondrial DNA replication during differentiation of murine embryonic stem cells. *Journal of Cell Science*, *120*, 4025–4034.

Fang, D., Yan, S., Yu, Q., Chen, D., & Yan, S. S. (2016). Mfn2 is required for mitochondrial development and synapse formation in human induced pluripotent stem cells/hiPSC derived cortical neurons. *Scientific Reports*, *6*, 31462.

Figge, M. T., Reichert, A. S., Meyer-Hermann, M., & Osiewacz, H. D. (2012). Deceleration of fusion-fission cycles improves mitochondrial quality control during aging. *PLoS Computational Biology*, *8*, e1002576.

Fike, J. R., Rosi, S., & Limoli, C. L. (2009). Neural precursor cells and central nervous system radiation sensitivity. *Seminars in Radiation Oncology*, *19*, 122–132.

Forsberg, K., Wuttke, A., Quadrato, G., Chumakov, P. M., Wizenmann, A., & Di Giovanni, S. (2013). The tumor suppressor p53 fine-tunes reactive oxygen species levels and neurogenesis via PI3 kinase signaling. *The Journal of Neuroscience*, *33*, 14318–14330.

Geschwind, D. H., Ou, J., Easterday, M. C., Dougherty, J. D., Jackson, R. L., Chen, Z., Antoine, H., Terskikh, A., Weissman, I. L., Nelson, S. F., & Kornblum, H. I. (2001). A genetic analysis of neural progenitor differentiation. *Neuron*, *29*, 325–339.

Hashiguchi, K., & Zhang-Akiyama, Q. M. (2009). Establishment of human cell lines lacking mitochondrial DNA. *Methods in Molecular Biology*, *554*, 383–391.

Hayashi, J., Tanaka, M., Sato, W., Ozawa, T., Yonekawa, H., Kagawa, Y., & Ohta, S. (1990). Effects of ethidium bromide treatment of mouse cells on expression and assembly of nuclear-coded subunits of complexes involved in the oxidative phosphorylation. *Biochemical and Biophysical Research Communications*, *167*, 216–221.

Hofmann, A. D., Beyer, M., Krause-Buchholz, U., Wobus, M., Bornhauser, M., & Rodel, G. (2012). OXPHOS supercomplexes as a hallmark of the mitochondrial phenotype of adipogenic differentiated human MSCs. *PLoS One*, *7*, e35160.

Homem, C. C. F., Steinmann, V., Burkard, T. R., Jais, A., Esterbauer, H., & Knoblich, J. A. (2014). Ecdysone and mediator change energy metabolism to terminate proliferation in drosophila neural stem cells. *Cell*, *158*, 874–888.

Hong, Y., Kristiansen, C. K., Chen, A., Nido, G. S., Høyland, L. E., Ziegler, M., Sullivan, G. J., Bindoff, L. A., & Liang, K. X. (2023). POLG genotype influences degree of mitochondrial dysfunction in iPSC derived neural progenitors, but not the parent iPSC or derived glia. *Experimental Neurology*, *365*, 114429.

Iwata, R., Casimir, P., & Vanderhaeghen, P. (2020). Mitochondrial dynamics in postmitotic cells regulate neurogenesis. *Science*, *369*, 858–862.

Iwata, R., & Vanderhaeghen, P. (2021). Regulatory roles of mitochondria and metabolism in neurogenesis. *Current Opinion in Neurobiology*, *69*, 231–240.

Jahani-Asl, A., Pilon-Larose, K., Xu, W., MacLaurin, J. G., Park, D. S., McBride, H. M., & Slack, R. S. (2011). The mitochondrial inner membrane GTPase, optic atrophy 1 (Opa1), restores mitochondrial morphology and promotes neuronal survival following excitotoxicity. *The Journal of Biological Chemistry*, *286*, 4772–4782.

Kahroba, H., Ramezani, B., Maadi, H., Sadeghi, M. R., Jaberie, H., & Ramezani, F. (2020). The role of Nrf2 in neural stem/progenitors cells: From maintaining stemness and self-renewal to promoting differentiation capability and facilitating therapeutic application in neurodegenerative disease. *Ageing Research Reviews*, *65*, 101211.

Kelly, D. P., & Scarpulla, R. C. (2004). Transcriptional regulatory circuits controlling mitochondrial biogenesis and function. *Genes & Development*, *18*, 357–368.

Khacho, M., Clark, A., Svoboda, D. S., Azzi, J., MacLaurin, J. G., Meghaizel, C., Sesaki, H., Lagace, D. C., Germain, M., Harper, M. E., Park, D. S., & Slack, R. S. (2016). Mitochondrial dynamics impacts stem cell identity and fate decisions by regulating a nuclear transcriptional program. *Cell Stem Cell*, *19*, 232–247.

Khacho, M., Clark, A., Svoboda, D. S., MacLaurin, J. G., Lagace, D. C., Park, D. S., & Slack, R. S. (2017). Mitochondrial dysfunction underlies cognitive defects as a result of neural stem cell depletion and impaired neurogenesis. *Human Molecular Genetics*, *26*, 3327–3341.

King, M. P., & Attardi, G. (1989). Human cells lacking mtDNA: Repopulation with exogenous mitochondria by complementation. *Science*, *246*, 500–503.

King, M. P., & Attardi, G. (1996). Isolation of human cell lines lacking mitochondrial DNA. *Methods in Enzymology*, *264*, 304–313.

Kochan, S. M. V., Malo, M. C., Jevtic, M., Jahn-Kelleter, H. M., Wani, G. A., Ndoci, K., Pérez-Revuelta, L., Gaedke, F., Schäffner, I., Lie, D. C., Schauss, A., & Bergami, M. (2024). Enhanced mitochondrial fusion during a critical period of synaptic plasticity in adult-born neurons. *Neuron*, *112*(1997–2014), e1996.

Kristiansen, C. K., Chen, A., Hoyland, L. E., Ziegler, M., Sullivan, G. J., Bindoff, L. A., & Liang, K. X. (2022). Comparing the mitochondrial signatures in ESCs and iPSCs and their neural derivations. *Cell Cycle*, *21*, 2206–2221.

Kukat, C., Wurm, C. A., Spahr, H., Falkenberg, M., Larsson, N. G., & Jakobs, S. (2011). Super-resolution microscopy reveals that mammalian mitochondrial nucleoids have a uniform size and frequently contain a single copy of mtDNA. *Proceedings of the National Academy of Sciences of the United States of America*, *108*, 13534–13539.

Kuroda, R., Tominaga, K., Kasashima, K., Kuroiwa, K., Sakashita, E., Hayakawa, H., Kouki, T., Ohno, N., Kawai, K., & Endo, H. (2021). Loss of mitochondrial transcription factor a in neural stem cells leads to immature brain development and triggers the activation of the integral stress response in vivo. *PLoS One*, *16*, e0255355.

Kuroiwa, T., Ohta, T., Kuroiwa, H., & Shigeyuki, K. (1994). Molecular and cellular mechanisms of mitochondrial nuclear division and mitochondriokinesis. *Microscopy Research and Technique*, *27*, 220–232.

Kuthethur, R., Shukla, V., Mallya, S., Adiga, D., Kabekkodu, S. P., Ramachandra, L., Saxena, P. U. P., Satyamoorthy, K., & Chakrabarty, S. (2022). Expression analysis and function of mitochondrial genome-encoded microRNAs. *Journal of Cell Science*, *135*, 1–15.

Lee, W., Johnson, J., Gough, D. J., Donoghue, J., Cagnone, G. L. M., Vaghjiani, V., Brown, K. A., Johns, T. G., & St. John, J. C. (2015). Mitochondrial DNA copy number is regulated by DNA methylation and demethylation of POLGA in stem and cancer cells and their differentiated progeny. *Cell Death & Disease*, *6*, e1664.

Legros, F., Malka, F., Frachon, P., Lombes, A., & Rojo, M. (2004). Organization and dynamics of human mitochondrial DNA. *Journal of Cell Science*, *117*, 2653–2662.

Li, M., Pevny, L., Lovell-Badge, R., & Smith, A. (1998). Generation of purified neural precursors from embryonic stem cells by lineage selection. *Current Biology*, *8*, 971–974.

Liang, H. L., Ongwijitwat, S., & Wong-Riley, M. T. (2006). Bigenomic functional regulation of all 13 cytochrome c oxidase subunit transcripts in rat neurons in vitro and in vivo. *Neuroscience*, *140*, 177–190.

Liang, K. X., Kristiansen, C. K., Mostafavi, S., Vatne, G. H., Zantingh, G. A., Kianian, A., Tzoulis, C., Høyland, L. E., Ziegler, M., Perez, R. M., Furriol, J., Zhang, Z., Balafkan, N., Hong, Y., Siller, R., Sullivan, G. J., & Bindoff, L. A. (2020). Disease-specific phenotypes in iPSC-derived neural stem cells with POLG mutations. *EMBO Molecular Medicine*, *12*, e12146.

Liu, H., Lu, J., He, Y., Yuan, B., Li, Y., & Li, X. (2014). Insulin-like growth factor-1 prevents dorsal root ganglion neuronal tyrosine kinase receptor expression alterations induced by dideoxycytidine in vitro. *Cellular and Molecular Neurobiology*, *34*, 183–194.

Livak, K. J., & Schmittgen, T. D. (2001). Analysis of relative gene expression data using real-time quantitative PCR and the 2(-Delta Delta C(T)) method. *Methods*, *25*, 402–408.

Lonergan, T., Brenner, C., & Bavister, B. (2006). Differentiation-related changes in mitochondrial properties as indicators of stem cell competence. *Journal of Cellular Physiology*, *208*, 149–153.

Lozoya, O. A., Xu, F., Grenet, D., Wang, T., Stevanovic, K. D., Cushman, J. D., Hagler, T. B., Gruzdev, A., Jensen, P., Hernandez, B., Riadi, G., Moy, S. S., Santos, J. H., & Woychik, R. P. (2021). A brain-specific pgc1alpha fusion transcript affects gene expression and behavioural outcomes in mice. *Life Science Alliance*, *4*, 1–17.

Mao, C. C., & Holt, I. J. (2009). Clinical and molecular aspects of diseases of mitochondrial DNA instability. *Chang Gung Medical Journal*, *32*, 354–369.

McBride, H. M., Neuspiel, M., & Wasiak, S. (2006). Mitochondria: More than just a powerhouse. *Current Biology*, *16*, R551–R560.

Metallo, C. M., & Vander Heiden, M. G. (2013). Understanding metabolic regulation and its influence on cell physiology. *Molecular Cell*, *49*, 388–398.

Montoya, J., Perez-Martos, A., Garstka, H. L., & Wiesner, R. J. (1997). Regulation of mitochondrial transcription by mitochondrial transcription factor a. *Molecular and Cellular Biochemistry*, *174*, 227–230.

Morais, R., Gregoire, M., Jeannotte, L., & Gravel, D. (1980). Chick embryo cells rendered respiration-deficient by chloramphenicol and ethidium bromide are auxotrophic for pyrimidines. *Biochemical and Biophysical Research Communications*, *94*, 71–77.

Nesti, C., Pasquali, L., Vaglini, F., Siciliano, G., & Murri, L. (2007). The role of mitochondria in stem cell biology. *Bioscience Reports*, *27*, 165–171.

Oswald, M. C. W., Garnham, N., Sweeney, S. T., & Landgraf, M. (2018). Regulation of neuronal development and function by ROS. *FEBS Letters*, *592*, 679–691.

Peterson, K. M., Aly, A., Lerman, A., Lerman, L. O., & Rodriguez-Porcel, M. (2011). Improved survival of mesenchymal stromal cell after hypoxia preconditioning: Role of oxidative stress. *Life Sciences*, *88*, 65–73.

Qi, Y., Ye, Y., Wang, R., Yu, S., Zhang, Y., Lv, J., Jin, W., Xia, S., Jiang, W., Li, Y., & Zhang, D. (2022). Mitochondrial dysfunction by TFAM depletion disrupts self-renewal and lineage differentiation of human PSCs by affecting cell proliferation and YAP response. *Redox Biology*, *50*, 102248.

Saccone, C., Gissi, C., Lanave, C., Larizza, A., Pesole, G., & Reyes, A. (2000). Evolution of the mitochondrial genetic system: An overview. *Gene*, *261*, 153–159.

Satoh, M., & Kuroiwa, T. (1991). Organization of multiple nucleoids and DNA molecules in mitochondria of a human cell. *Experimental Cell Research*, *196*, 137–140.

Scarpulla, R. C. (2002a). Nuclear activators and coactivators in mammalian mitochondrial biogenesis. *Biochimica et Biophysica Acta*, *1576*, 1–14.

Scarpulla, R. C. (2002b). Transcriptional activators and coactivators in the nuclear control of mitochondrial function in mammalian cells. *Gene*, *286*, 81–89.

Scarpulla, R. C. (2008a). Nuclear control of respiratory chain expression by nuclear respiratory factors and PGC-1-related coactivator. *Annals of the new York Academy of Sciences*, *1147*, 321–334.

Scarpulla, R. C. (2008b). Transcriptional paradigms in mammalian mitochondrial biogenesis and function. *Physiological Reviews*, *88*, 611–638.

Silva Ramos, E., Motori, E., Bruser, C., Kühl, I., Yeroslaviz, A., Ruzzenente, B., Kauppila, J. H. K., Busch, J. D., Hultenby, K., Habermann, B. H., Jakobs, S., Larsson, N.-G., & Mourier, A. (2019). Mitochondrial fusion is required for regulation of mitochondrial DNA replication. *PLoS Genetics*, *15*, e1008085.

Soares, R., Lourenco, D. M., Mota, I. F., Sebastiao, A. M., Xapelli, S., & Morais, V. A. (2024). Lineage-specific changes in mitochondrial properties during neural stem cell differentiation. *Life Science Alliance*, *7*, 1–15.

Souder, D. C., Mcgregor, E. R., Rhoads, T. W., Clark, J. P., Porter, T. J., Eliceiri, K., Moore, D. L., Puglielli, L., & Anderson, R. M. (2023). Mitochondrial regulator PGC-1a in neuronal metabolism and brain aging. *bioRxiv*, 1–27.

St John, J. C., Ramalho-Santos, J., Gray, H. L., Petrosko, P., Rawe, V. Y., Navara, C. S., Simerly, C. R., & Schatten, G. P. (2005). The expression of mitochondrial DNA transcription factors during early cardiomyocyte in vitro differentiation from human embryonic stem cells. *Cloning and Stem Cells*, *7*, 141–153.

Uittenbogaard, M., Brantner, C. A., & Chiaramello, A. (2018). Epigenetic modifiers promote mitochondrial biogenesis and oxidative metabolism leading to enhanced differentiation of neuroprogenitor cells. *Cell Death & Disease*, *9*, 360.

Van Den Ameele, J., & Brand, A. H. (2019). Neural stem cell temporal patterning and brain tumour growth rely on oxidative phosphorylation. *eLife*, *8*, 1–20.

Verma, M., Francis, L., Lizama, B. N., Callio, J., Fricklas, G., Wang, K. Z. Q., Kaufman, B. A., D'Aiuto, L., Stolz, D. B., Watkins, S. C., Nimgaonkar, V. L., Soto-Gutierrez, A., Goldstein, A., & Chu, C. T. (2023). iPSC-derived neurons from patients with POLG mutations exhibit decreased mitochondrial content and dendrite simplification. *The American Journal of Pathology*, *193*, 201–212.

Virbasius, J. V., & Scarpulla, R. C. (1994). Activation of the human mitochondrial transcription factor a gene by nuclear respiratory factors: A potential regulatory link between nuclear and mitochondrial gene expression in organelle biogenesis. *Proceedings of the National Academy of Sciences of the United States of America*, *91*, 1309–1313.

Viscomi, C., & Zeviani, M. (2017). MtDNA-maintenance defects: Syndromes and genes. *Journal of Inherited Metabolic Disease*, *40*, 587–599.

Wanet, A., Arnould, T., Najimi, M., & Renard, P. (2015). Connecting mitochondria, metabolism, and stem cell fate. *Stem Cells and Development*, *24*, 1957–1971.

Wang, G. J., Nutter, L. M., & Thayer, S. A. (1997). Insensitivity of cultured rat cortical neurons to mitochondrial DNA synthesis inhibitors: Evidence for a slow turnover of mitochondrial DNA. *Biochemical Pharmacology*, *54*, 181–187.

Wang, W., Esbensen, Y., Kunke, D., Suganthan, R., Rachek, L., Bjoras, M., & Eide, L. (2011). Mitochondrial DNA damage level determines neural stem cell differentiation fate. *The Journal of Neuroscience*, *31*, 9746–9751.

Wu, Z., Puigserver, P., Andersson, U., Zhang, C., Adelmant, G., Mootha, V., Troy, A., Cinti, S., Lowell, B., Scarpulla, R. C., & Spiegelman, B. M. (1999). Mechanisms controlling mitochondrial biogenesis and respiration through the thermogenic coactivator PGC-1. *Cell*, *98*, 115–124.

Xavier, J. M., Rodrigues, C. M., & Sola, S. (2016). Mitochondria: Major regulators of neural development. *The Neuroscientist*, *22*, 346–358.

Yang, X., Wu, J., Jing, S., Forster, M. J., & Yan, L. J. (2018). Mitochondrial protein sulfenation during aging in the rat brain. *Biophysical Reports*, *4*, 104–113.

Yu, J., Wang, P., Ming, L., Wood, M. A., & Zhang, L. (2007). SMAC/diablo mediates the proapoptotic function of PUMA by regulating PUMA-induced mitochondrial events. *Oncogene*, *26*, 4189–4198.

Yuan, H. X., Xiong, Y., & Guan, K. L. (2013). Nutrient sensing, metabolism, and cell growth control. *Molecular Cell*, *49*, 379–387.

Zehnder, T., Petrelli, F., Romanos, J., de Oliveira Figueiredo, E. C., Lewis, T. L., Jr., Déglon, N., Polleux, F., Santello, M., & Bezzi, P. (2021). Mitochondrial biogenesis in developing astrocytes regulates astrocyte maturation and synapse formation. *Cell Reports*, *35*, 108952.

Zhang, Y., Marsboom, G., Toth, P. T., & Rehman, J. (2013). Mitochondrial respiration regulates adipogenic differentiation of human mesenchymal stem cells. *PLoS One*, *8*, e77077.

Zheng, X., Boyer, L., Jin, M., Mertens, J., Kim, Y., Ma, L., Ma, L., Hamm, M., Gage, F. H., & Hunter, T. (2016). Metabolic reprogramming during neuronal differentiation from aerobic glycolysis to neuronal oxidative phosphorylation. *eLife*, *5*, 1–27.

Zhu, Y., Zhang, J. L., Yan, X. J., Ji, Y., & Wang, F. F. (2023). Exploring a new mechanism between lactate and VSMC calcification: PARP1/POLG/UCP2 signaling pathway and imbalance of mitochondrial homeostasis. *Cell Death & Disease*, *14*, 598.

SUPPORTING INFORMATION

Additional supporting information can be found online in the Supporting Information section at the end of this article.

How to cite this article: Walter-Manucharyan, M., Martin, M., Pfützner, J., Markert, F., Rödel, G., Deussen, A., Hermann, A., & Storch, A. (2024). Mitochondrial DNA replication is essential for neurogenesis but not gliogenesis in fetal neural stem cells. *Development, Growth & Differentiation*, *66*(8), 398–413. https://doi.org/10.1111/dgd.12946